Photolineaments in the ASTP Stereostrip of the Western Desert of Egypt

Hassan A. El-Etr,[a] Adel R. Moustafa,[a] and Farouk El-Baz[b†]

ABSTRACT

This paper deals with the study of photolineaments displayed on the Apollo-Soyuz stereostrip covering part of the Western Desert of Egypt. Photolineaments abound in the study area and are easily distinguished on the color photographs. Many of these photolineaments, which are soil-tonal or topographic alinements, are probably the surface expressions of faults or fractures. Others are most likely related to erosional escarpments at formational boundaries. Photolineaments in the Western Desert occurred most frequently in two regions: the Baharîya/Sitra region and the Qattara Depression/Wâdi el Natrûn region. The area between these two regions is probably blanketed by unconsolidated rock and/or active sand sheets. From this study, it is believed that there are two preferred regional orientations of the photolineaments: east-northeast to east-west and northwest to west-northwest.

A comparison of the detectability of photolineaments on Apollo-Soyuz photographs and Landsat images was made. Virtually all of the photolineaments detected on Landsat images (black-and-white as well as false-color composites) were also detected on Apollo-Soyuz photographs of the same scale and approximately the same resolution. In this study, the drawbacks of Apollo-Soyuz photographs include (1) the low base/height ratio, which limited the effective stereovision; (2) the high Sun-elevation angle, which limited the shadows required to easily identify linear features; and (3) the overexposure of the central parts of the frames, particularly over the Great Sand Sea. Recommendations are made to remedy this on future Earth-orbital photographic missions.

INTRODUCTION

As a primary objective of the Earth Observations and Photography Experiment on the Apollo-Soyuz Test Project (ASTP), a strip of 15 vertical photographs was taken over the Western Desert of Egypt. This strip was acquired from an altitude of approximately 220 km with a bracket-mounted 70-mm Hasselblad data camera using a 60-mm lens. The strip is oriented in a northeasterly direction, and it extends for approximately 1000 km from east of the Egyptian-Libyan border, near latitude 26°30′ N, to the Nile Delta near latitude 31°30′ N. The width of this strip is approximately 200 km.

The ASTP photographic strip is bounded on the northwestern side by the Sitra Depression and the northeastern part of the Qattara Depression; it reaches the Mediterranean Sea east of El 'Alamein. The southeastern side of the strip is bounded by the northwestern edge of the Farâfra and Baharîya oases; it extends across the Nile Delta south of Tanta and crosses the Mediterranean coast just west of Port Said. This report pertains to data obtained from 9 of the 15 photographs covering the stretch extending from northwestern Farâfra to west of the Nile Delta. The

[a]Ain Shams University, Cairo, Egypt.

[b]National Air and Space Museum, Smithsonian Institution.

[†]Principal Investigator.

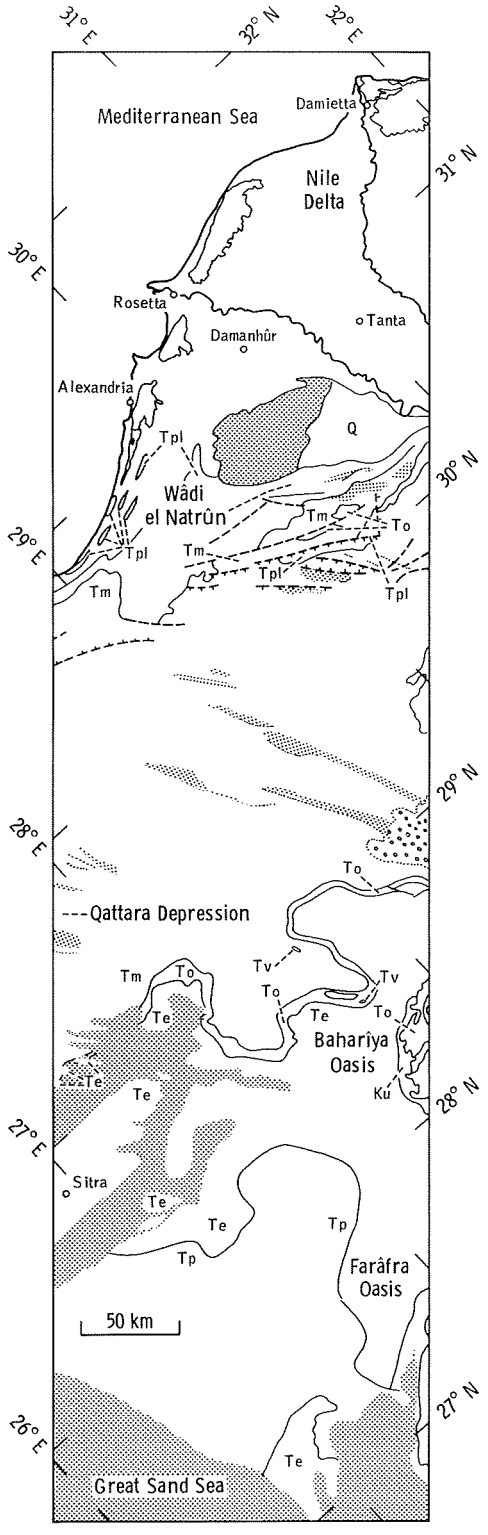

FIGURE 1.—Geological map of the Western Desert region covered by ASTP photographs and studied in this report (from ref. 1).

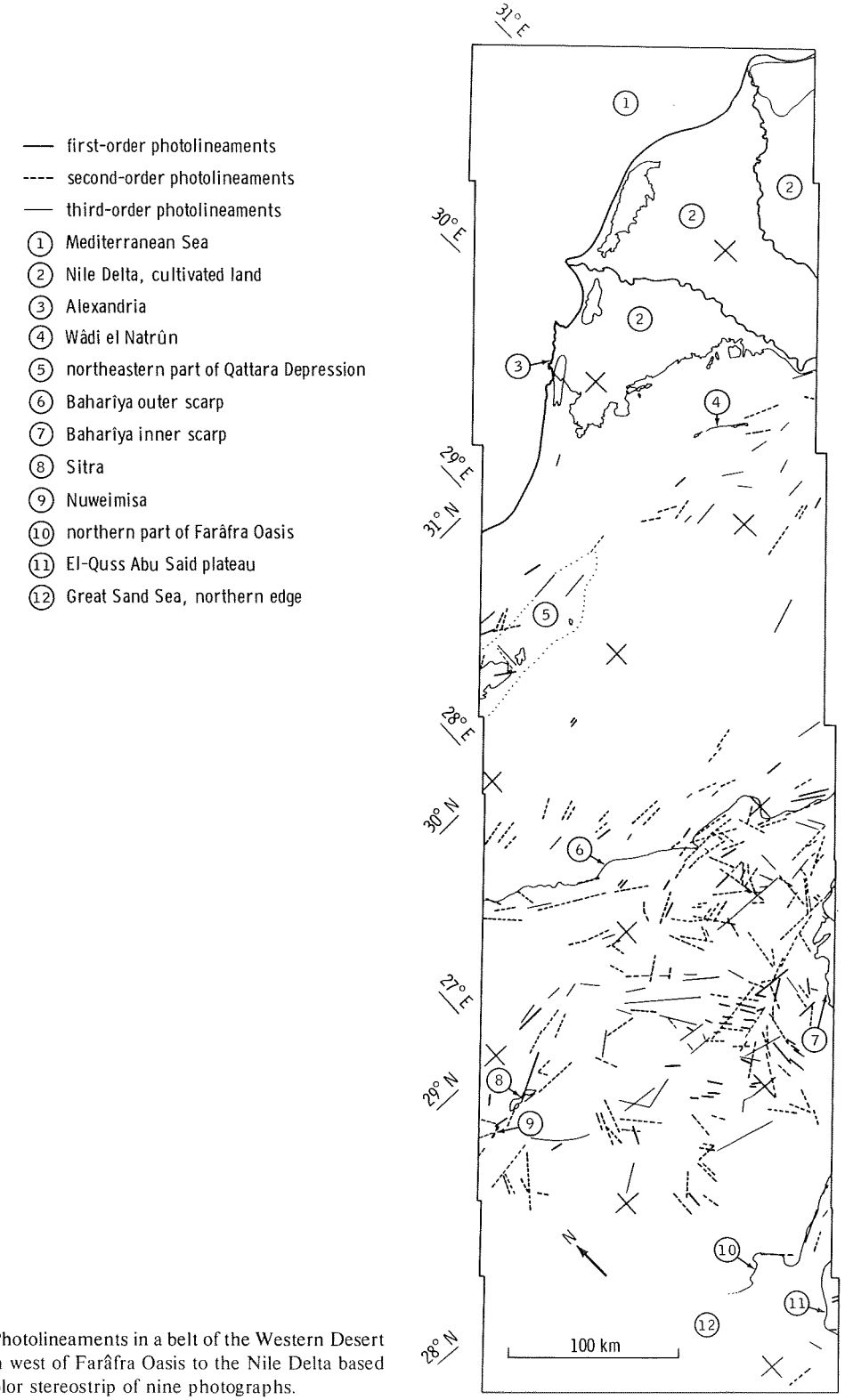

FIGURE 2.—Photolineaments in a belt of the Western Desert extending from west of Farâfra Oasis to the Nile Delta based on an ASTP color stereostrip of nine photographs.

photographs across the Great Sand Sea were not studied because they were overexposed.

The geology of this area is not well known (fig. 1; ref. 1). In general terms, the Western Desert is characterized by thick beds of sedimentary rocks that dip gently to the north and that decrease in age from south to north. Detailed geological and structural maps exist only for the northern part of the area (ref. 2). The southern half of the area is comparatively unexplored. For this reason, the study of the ASTP photographs supplemented by Landsat images could add much to our knowledge of the structural setting of the area.

PHOTOLINEAMENTS

Photolineament (ref. 3) is a term that has been used to describe natural linear features of any length that appear on photographs. This definition includes topographic, physiographic (straight stream segments), lithologic, structural, vegetational, and soil-tonal alinements, or any combinations thereof. More specifically, according to El-Etr (ref. 3), these lineaments may be subdivided and classified by length into megalineaments (>100 km), lineaments (100 to 10 km), macrolineaments (10 to 2 km), brachylineaments (2 km or less), and microlineaments (below the resolution limit of the unaided eye). The last three divisions may be referred to by the general term 'linear' (<10 km).

The advent of the space age has provided a new dimension to the study of photolineaments. Photographs obtained from Earth orbit provide a powerful tool for the direct identification of regional and super-regional structures. These structures become visible in a single space photograph as compared with aerial views that require mosaics of hundreds of aerial photographs. In addition, the orbital photographs enable correlations to be made between geographically separated structures.

The technique of quantitative analysis of photolineaments has previously been discussed and reviewed (ref. 4). Briefly, each photograph is viewed in eight different directions, four parallel to its sides and four diagonal to these. The light source remains fixed and is always high behind the analyst's left shoulder. The detected photolineaments are marked on the photographs using a grease pencil. Reliability orders are then assigned; the first order denotes the most pronounced photolineaments and the third order the most subtle.

The photolineament pattern is usually checked after several days to identify any linear features that may have been missed during earlier stages. During this checking stage, the reliability ordering is reevaluated.

Because the ASTP strip was taken with 60 percent overlap, successive photographs could be viewed stereoscopically. The stereoscopic viewing provided an additional capability to confirm both major and minor photolineaments.

The next phase of the study includes the compilation of the photolineaments on a map and their analysis. Each linear feature is annotated; its length in kilometers and its orientation (azimuth) in classes of 10° of arc are determined. Grid units are laid over the maps to count the number of photolineaments per unit area. Frequency curves are constructed for the number in percent (N%) and length in percent (L%) of photolineaments in each grid unit area. Gay's suggestions (ref. 5) for drawing frequency curves are followed. Also, the Poisson frequency distribution statistical method (ref. 6) is applied to test the significance of the peaks obtained at the 95-percent level and to show the areal variations in photolineament density.

Use of the previously described procedure led to the stereoscopic detection of 307 linear features (fig. 2), of which 135 rank as "lineaments" (10 km or longer) and 172 rank as "linears" (shorter than 10 km). Many of the photolineaments do not correspond to faults or structures shown on the 1971 geologic map of Egypt (compare figs. 1 and 2) (ref. 1).

As previously stated, the detected photolineaments were classified into three orders of reliability. Two hundred and fifty photolineaments belong to the first and second orders; 108 of these are lineaments and 142 are linears. The remaining photolineaments belong to the third order and include 27 lineaments and 30 linears. The orientation and length of these photolineaments per 10° classes of azimuth are included in table I.

The photolineament pattern shown in figure 2 includes a conspicuous concentration in the Baharîya/Sitra region and a less dense concentration in the Qattara Depression/Wâdi el Natrûn region. The areas in between are generally low in photolineament concentration. This low density is attributed to partial or total masking of bedrock exposures by unconsolidated sediments (mainly sand dunes, sand sheets, and "serir," or pebble-strewn desert plains). Another reason for the association of photolineaments and depressions such as Baharîya, Sitra, Qattara, and Wâdi el Natrûn may be that the depressions are structurally controlled.

Study of figure 2 shows that the photolineament patterns have prominent east-northeasterly and northwesterly trends. For a quantitative analysis of the frequencies of photolineament trends, six frequency curves were plotted (fig. 3). The Group I plots represent frequency curves of the numbers and lengths in percent of the selective field of first- and second-order photolineaments (I-1), the selective field of the third order (I-2), and the total field (first, second, and third order) photolineaments (I-3).

The peaks detected in plot I-1, in decreasing statistical significance, are ENE, NW, WNW, and NNE. Those detected in plot I-2 are more differentiated, with less background photolineament scattering, and are as follows: E-W, NW to WNW, and NNE. The average length of linear features of the third order is relatively more than that of linear features of the first and second orders. This difference seems plausible because the longer a photolineament is, the more subtle and complex its appearance on photographs; hence, its

TABLE I.—Photolineaments Detected in Area Covered by ASTP Stereostrip of Western Desert

(a) Northwesterly

Parameter (a)	*Photolineaments with orientation, deg, of—*								
	81-[b]90	*71-80*	*61-70*	*51-60*	*41-50*	*31-40*	*21-30*	*11-20*	*[c]0-10*
					First and second orders				
N.....	18	8	20	13	23	20	9	11	11
N, percent .	7.2	3.2	8.0	5.2	9.2	8.0	3.6	4.4	4.4
L, km	225.6	70.0	244.4	141.1	218.9	195.6	88.9	102.2	107.8
L, percent..	8.0	2.5	8.6	5.0	7.7	6.9	3.1	3.6	3.8
					Third order				
N.....	9	2	4	5	5	5	3	1	1
N, percent .	15.8	3.5	7.0	8.8	8.8	8.9	5.3	1.8	1.8
L, km	153.3	60.0	43.3	94.4	40.0	73.3	27.8	7.8	12.2
L, percent..	20.4	8.0	5.8	12.6	5.3	9.7	3.7	1.0	1.6
					Total				
N.....	27	10	24	18	28	25	12	12	12
N, percent .	8.8	3.3	7.9	5.9	9.1	8.1	3.9	3.9	3.9
L, km	378.9	130.0	287.7	235.5	258.9	268.9	116.7	110.0	120.0
L, percent..	10.6	3.6	8.0	6.6	7.2	7.5	3.3	3.1	3.3

[a]N = number of photolineaments; L = total length of photolineaments.
[b]90° = west.
[c]0° = north.

TABLE I.—Concluded

(b) Northeasterly

Parameter (a)	*Photolineaments with orientation, deg, of —*								
	[c]*0-10*	*11-20*	*21-30*	*31-40*	*41-50*	*51-60*	*61-70*	*71-80*	*81-*[d]*90*
					First and second orders				
N.....	13	8	10	8	4	10	11	28	25
N, percent .	5.2	3.2	4.0	3.2	1.6	4.0	4.4	11.2	10.0
L, km	175.6	88.9	113.3	101.1	38.9	115.6	160.0	348.9	298.9
L, percent .	6.2	3.1	4.0	3.6	1.4	4.1	5.6	12.3	10.5
					Third order				
N.....	2	1	-	-	2	2	2	5	8
N, percent .	3.5	1.8	-	-	3.5	3.5	3.5	8.9	14.0
L, km	14.4	4.4	-	-	26.7	40.0	15.6	57.8	81.1
L, percent .	1.9	0.6	-	-	3.5	5.3	2.1	7.7	10.8
					Total				
N.....	15	9	10	8	6	12	13	33	33
N, percent .	4.9	2.9	3.3	2.6	2.0	3.9	4.2	10.7	10.7
L, km	190.0	93.3	113.3	101.1	65.6	155.6	175.6	406.7	380.0
L, percent .	5.3	2.6	3.2	2.8	1.9	4.3	4.9	11.3	10.6

[a]N = number of photolineaments; L = total length of photolineaments.
[c]0° = north.
[d]90° = east.

(c) Grand total

Ordering	*Number*	*Length, km*
First and second	250	2835.7
Third	57	752.1
Total	307	3587.8

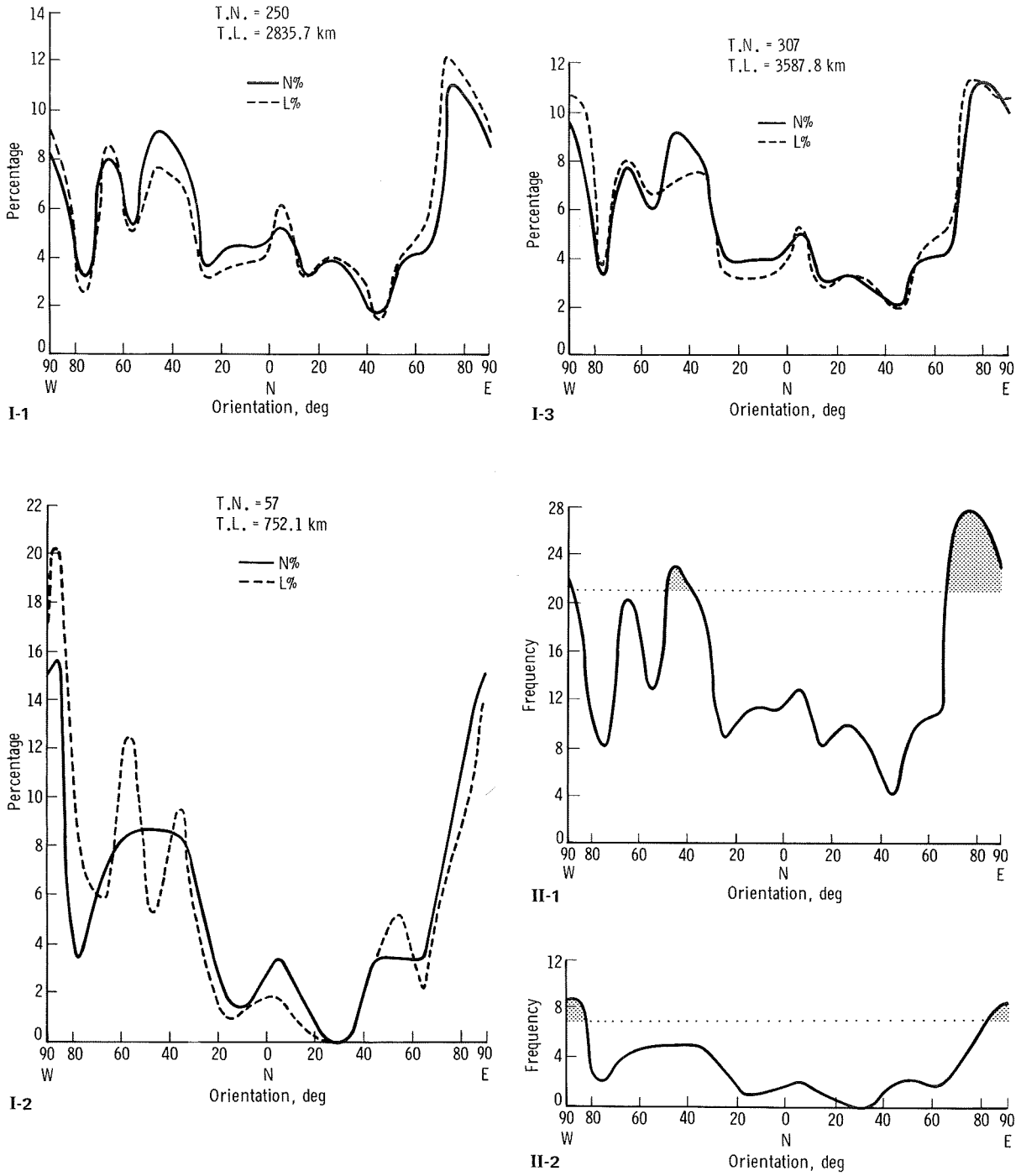

FIGURE 3.—Frequency curves of ASTP photolineaments in the area covered by the stereostrip. Diagrams in Group I are based on number in percent (N%) and length in percent (L%). Total numbers (T.N.) and total lengths (T.L.) are also given. Diagrams in Group II are based on the total number of photolineaments. Diagrams I-1 and II-1 include photolineaments of the first and second orders; diagrams I-2 and II-2 include photolineaments of the third order; and diagrams I-3 and II-3 are summations for photolineaments of the first, second, and third orders. Dotted horizontal lines in type II diagrams delimit the significant peaks calculated using the Poisson frequency distribution at the 95-percent significance level.

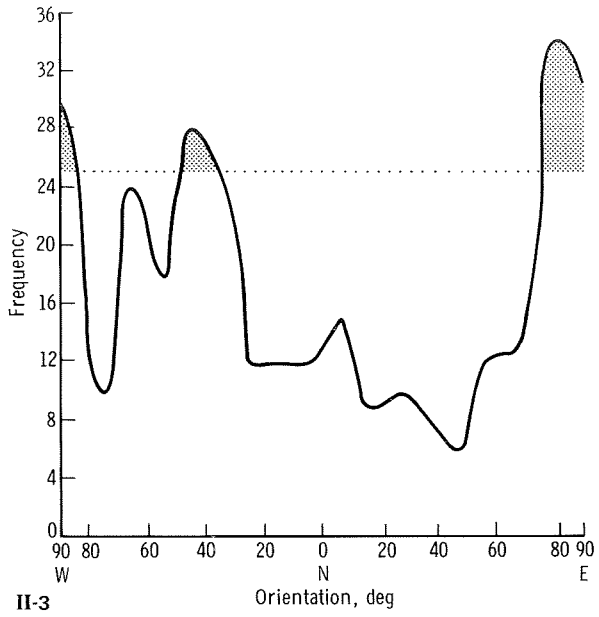

FIGURE 3.—Concluded.

low reliability ranking. It should be mentioned, however, that plot I-2 is based on a relatively smaller number of photolineaments (57) than that on which plot I-1 is based (250). Plot I-3 is a summation of plots I-1 and I-2. The peaks illustrated, in decreasing order, are ENE to E-W, NW to WNW, and NNE.

The azimuth-frequency distribution of the 307 linear features of the region was statistically tested using the Poisson frequency distribution (ref. 6). The Group II plots in figure 3 represent frequency curves based on actual numbers of photolineaments for first- and second-order photolineaments (II-1), third-order photolineaments (II-2), and their total field (II-3). The dotted horizontal line delimits the peaks that are significant at the 95-percent significance level. Diagram II-1 shows two such peaks, oriented ENE and NW. Diagram II-2, however, shows only one peak, oriented E-W (although split in two sectors). The summation diagram, II-3, shows the prominence of the regional trends ENE to E-W and NW to WNW; thus confirming the results obtained from the Group I frequency curves. It becomes evident, also, that the ENE trend is of local significance only.

DISCUSSION

Photolineaments were easily detected on the ASTP color photographs. Many of these photolineaments are probably the surface expressions of faults or fractures. Others are most likely related to erosional escarpments at formational boundaries. The photolineaments are mainly clustered in the Baharîya/Sitra region and the Qattara Depression/Wâdi el Natrûn region. The presence of photolineaments in these two regions seems to indicate that structural control played a part in the formation of the main depressions in the region. The absence of photolineaments between these two areas is attributed to partial or total masking of bedrock by unconsolidated material.

There is a specific preferred regional orientation of the photolineaments of the Western Desert of Egypt. These orientations are ENE to E-W and NW to WNW.

In the present study, virtually all photolineaments detected on Landsat images were also detected on the ASTP photographs. A few photolineaments detected on Landsat images were refuted, however, after a check of the ASTP photographs showed that they were superfluous lines related to imperceptible cloud alinements and the like. On the other hand, a few linear features detected on Landsat images are subtle or indistinct on their ASTP counterparts. This is attributed mainly to the broader electromagnetic spectrum involved in Landsat imagery (particularly the near-infrared band 7).

Being in natural colors, ASTP photographs are more easily interpreted than black-and-white photographs or single-band Landsat images. Alterations, weathering manifestations, and bedrock colors are the same as observed on the ground. This is a rather distinct advantage over multispectral false-color images, such as those produced by Landsat, which need a "mental translation" of each electronic color into the corresponding natural color.

The photographic texture is clear by comparison with the electronically assembled images of the Landsat type. Flaws in the linear electronic runs in Landsat images commonly occur and may be misidentified as natural linear features. For the

ASTP photographic strip, although stereovision was achieved using ordinary mirror stereoscopes, depth perception was rather limited because of the inherent low relief of the region; modification of the base/height ratio of stereophotographs may be deemed necessary to enhance the vertical exaggeration. The effective resolution of the stereostrip photographs needs to be increased; this need was particularly felt during field and aerial photographic checking of the dune forms in the region.

The ASTP photographs taken over the central Western Desert suffered from a high Sun-elevation angle and from the overexposure of the centers of some photographs. This characteristic is generally referred to as vignetting. More effective antivignetting filters should be used in future flights. Vignetting is a gradual reduction in density of parts of a photographic image caused by the stopping of some rays entering the lens (ref. 7). Thus, a lens mounting may interfere with the extremely oblique rays. An antivignetting filter is one that gradually decreases in density from the center toward the edges; it is used with aerial wide-angle lenses to produce a photograph of uniform density by reducing the overexposure of the photograph center.

ACKNOWLEDGMENTS

Part of the research was done in partial fulfillment of the requirements for the degree of Master of Science for the second author (ref. 8). The report was prepared under both the Ain Shams University/Smithsonian Institution joint research project and NASA contract NAS9-13831.

REFERENCES

1. Geological Map of Egypt, Scale 1:2 000 000. Geological Survey of Egypt, 1971.

2. Said, Rushdi: The Geology of Egypt. Elsevier Pub. Co. (Amsterdam), 1962.

3. El-Etr, H. A.: Proposed Terminology of Natural Linear Features. Proceedings of the First International Conference on the New Basement Tectonics, Utah Geol. Assoc., no. 5, 1976, pp. 480-489.

4. El-Etr, H. A.; and Abdel-Rahman, M. A.: Air Photo Lineations of the Southern Part of the Gulf of Suez Region, Egypt. Proceedings of the First International Conference on the New Basement Tectonics, Utah Geol. Assoc., no. 5, 1976, pp. 309-326.

5. Gay, S. Parker, Jr.: Standardization of Azimuthal Presentations. Proceedings of the First International Conference on the New Basement Tectonics, Utah Geol. Assoc., no. 5, 1976, pp. 499-500.

6. Hay, A. M.; and Abdel-Rahman, M. A.: Use of Chi-Square for the Identification of Peaks in Orientation Data: A Comment. Bull. Geol. Soc. America, vol. 85, Dec. 1974, pp. 1963-1965.

7. Smith, John T., Jr., ed.: Manual of Color Aerial Photography. American Soc. Photogram. (Arlington, Va.), 1968.

8. Moustafa, A. R.: Photogeology of the Central Western Desert, Egypt (With a Special Emphasis on Siwa and Bahariya Oases). M. S. Thesis, Ain Shams University (Cairo, Egypt), 1977.